Appl Phys B (2010) 99: 385–390
DOI 10.1007/s00340-010-3980-3

Applied Physics B
Lasers and Optics

RAPID COMMUNICATION

Simultaneous measurement of liquid water film thickness and vapor temperature using near-infrared tunable diode laser spectroscopy

H. Yang · D. Greszik · T. Dreier · C. Schulz

Received: 7 October 2009 / Revised version: 20 February 2010 / Published online: 19 March 2010

Abstract A fiber-based multiplexed tunable diode-laser absorption sensor with three near-infrared distributed-feedback diode lasers at ∼1.4 μm is used for simultaneous nonintrusive measurements of liquid water film thickness and vapor-phase temperature. Water film thicknesses are derived from broad-band absorption determined at two fixed wavelengths while gas-phase temperature above the film is obtained via two-line thermometry using the fast wavelength tuning with line-integrating absorption. Probing the liquid film at two wavelengths with significantly different liquid-phase absorption cross sections allows discriminating against additional signal losses due to surface fowling, reflection, and beam steering. The technique is demonstrated for liquid layers of defined thicknesses and in time-resolved measurements of evaporating films.

1 Introduction

Liquid-film formation and evaporation is relevant in many practical applications. For optimizing the operation of devices and to provide validation data for simulations, quantitative measurement techniques of liquid-film thickness are required. Significant work has been published for the measurement of fuel films, e.g., in internal combustion engines such as at the inner walls of the inlet port in port-injected gasoline engines (e.g., Ref. [1]), on piston heads in direct-injection spark-ignition (DISI) engines (e.g., Ref. [2]), in the intake manifold during cold start [3]. Water-based films are of interest in film cooling [4], shear-driven films in turbulent gases [5], fire suppression [6], etc. In engine-related applications the observation of the dynamic behavior of liquid water films is of interest during injection of water–urea solutions into the exhaust pipe for selective catalytic reduction (SCR) of NO_x [7].

Several optical techniques have been used to measure liquid-film thicknesses before. Some of these make use of the intensity of the totally and partially reflected light inside the film as a measurement of film thickness [8]. The technique of total internal reflection which occurs at a liquid–vapor interface due to the refractive index difference between a liquid and a vapor is also used by Hurlburt et al. [8]. Film thicknesses are measured in a triangulation scheme where the lateral displacement of a laser beam reflected back from the liquid layer is observed by a camera. Instead of a laser Shedd et al. [9] sent light from a LED through the film-covered wall and also determined the displacement of the beam. Spectroscopic methods have been used for the measurement of fluid-film thickness: The fluorescence emitted from hydrocarbon fuel films after excitation in the ultraviolet was exploited by Kull et al. for two-dimensional imaging [10]. Greszik et al. used a combination of laser-induced fluorescence (LIF) and spontaneous Raman scattering for imaging water film thickness [11]. The absorption of a blue laser light in a dyed liquid was employed by Mouza et al. [12] to measure the thickness of flowing films. Porter et al. [13] used the strong absorption of hydrocarbon fuels in the Mid-IR at around 3.3 μm, while the absorption of near-infrared (NIR) emission from a He–Ne laser was used by Wittig et al. [14] to study the wall film behavior in the suction pipes of SI engines.

In this paper we demonstrate the use of a scanning, multiplexed near-infrared diode laser absorption spectrometer for the measurement of the thickness of liquid water films and

H. Yang (✉) · D. Greszik · T. Dreier · C. Schulz
IVG, Universität Duisburg-Essen, Lotharstr. 1, 47057 Duisburg, Germany
e-mail: huinan.yang@uni-due.de
Fax: +49-203-3793087

the temporally resolved simultaneous measurement of film thickness and water-vapor temperature above the evaporating liquid. The influence of liquid-phase temperature on the water film thickness measurement is also investigated.

2 Measurement strategies

Tunable diode laser absorption spectroscopy (TDLAS) has been used before for vapor-phase concentration and temperature measurements of water in a wide variety of applications (e.g., Ref. [15]). When evaluating the absorption strength on two or more rovibrational transitions in the overtone or combination bands in the NIR region, temperatures can be derived over a range depending on the temperature sensitivity of the chosen transitions [16, 17].

In the liquid phase, due to van der Waals hydrogen bridge bonding and hindered rotations water exhibits broad-band absorption from the OH-stretch vibrational bands within the same spectral range. A review of the absorption spectrum of liquid water covering the wavelength region between 0.2 and 200 µm is given by Hale et al. [18] and a more detailed compilation in the 0.65–2.5 µm range is presented by Kou et al. [19]. The absorption spectrum of liquid water for the wavelength range relevant for our work also has been reported in Ref. [20] for a number of different temperatures.

TDLAS relies on a rapid scanning of the laser wavelength via current tuning to distinguish between narrow band molecular absorption features in the gas phase and laser attenuation due to other losses such as reflection at interfaces, window fouling, scattering, and beam steering. The molecular absorption is then derived from the spectrally integrated narrowband absorption features after subtracting the spectrally unstructured background effects. When a liquid–water film is present in the beam path, additional broad-band absorption originating from the overtone vibrational bands in the liquid occurs. Its contribution is suppressed in data evaluation when determining line-integrated absorption. The data evaluation, however, also returns information about the broad-band absorption. Because in the 1.3–1.5 µm range the broad-band absorption of liquid water is strongly wavelength dependent a measurement at two (or more) wavelengths allows separating the absorption due to liquid water from the other light losses that can be considered wavelength independent. The liquid–water absorption spectrum changes with temperature (cf. [20]) with a clever choice of a third wavelength, a simultaneous measurement of liquid film thickness and liquid-phase temperature in the presence of unspecific laser attenuation is thus possible.

In our experiments we use a combination of diode lasers to (1) separate the liquid-film absorption from the background and (2) to provide a suitable wavelength pair for sensitive gas-phase thermometry. Theoretically, two laser wavelengths would be sufficient. To use optimized wavelength combinations for both the liquid film and the gas-phase temperature measurements, however, we apply three different lasers. The lasers used in our work are listed in Table 1 with their respective center wavenumber positions and fractional absorptions for a typical liquid film thickness of 100 µm, and saturated water vapor with 1-cm absorption length at room temperature, respectively. The lasers are operated both in fixed- and scanned-wavelength mode. If only liquid film thickness measurements are of interest, fixed-wavelength spectroscopy with a simplified setup is sufficient. In this case, the lasers are tuned to wavelength positions that are not in resonance with any water vapor absorption lines to avoid biasing the results due to vapor phase absorption in ambient air.

Table 1 Properties of the diode lasers used and fractional absorption values expected for typical measurement situations

Laser	Center wavenumber position (cm^{-1})	Fractional absorption in 100 µm liquid water (25°C)	Fractional peak absorption in 1 cm saturated water vapor (25°C)
1	6807.83	24.9%	0.068%
2	7185.59	8.5%	3.48%
3	7390.13	1.5%	6.35%

Because there are no accurate liquid–water absorption cross sections available in Ref. [20] for the exact wavenumber positions of the lasers used in our work, own measurements were made using a Fourier-transform infrared (FTIR) spectrometer with a spectral resolution of 2 cm^{-1}. Tridistilled liquid water was measured in a 1-mm-path-length quartz cuvette that is heated to temperatures between 25 and 75°C with circulating heated oil. Figure 1 presents the absorption spectrum at various temperatures from 5800 to 7800 cm^{-1}. From repeated measurements an instrumental accuracy of 1% can be stated with respect to absorption cross sections and wavelength dependence of the depicted spectral band. The center wavenumber positions of the three diode lasers used in the current experiments are indicated as vertical lines in Fig. 1. The absorption cross section at the wavelength of laser 1 is approximately ten times larger compared to that of laser 3 thus allowing to discriminate between the water absorption and the background attenuation.

The liquid–water absorption feature shifts towards shorter wavelengths with increasing temperature causes increasing absorption of lasers 2 and 3 but decreasing absorption of laser 1, thus allowing for liquid temperature measurements from the ratio of two absorption signals in the absence of background attenuation or from three wavelength in a typical case where an unknown contribution from unspecific attenuation is present.

Scanned-wavelength spectroscopy allows the simultaneous determination of liquid phase absorption and gas phase

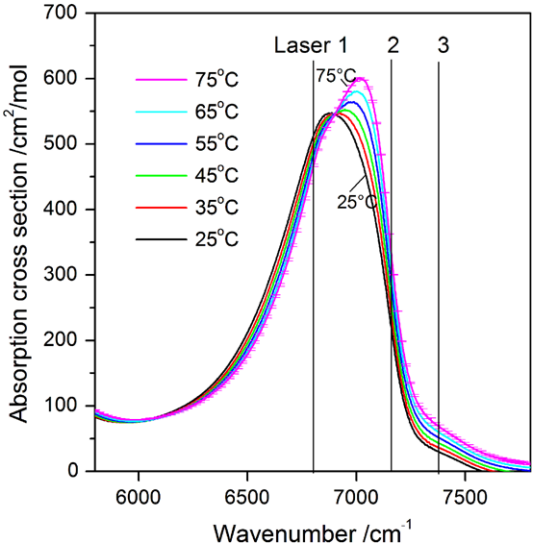

Fig. 1 Near-infrared absorption spectrum of liquid water for temperatures between 25 and 75°C measured via FTIR

temperature. In that case, laser 1 is tuned to a wavelength not in resonance with any water vapor transition, while lasers 2 and 3 are tuned across the vapor phase absorption lines accessible with the current laser sources. Their difference in ground state energies allows sensitive temperature measurements in the 300–700 K range [21]. After subtracting the narrow band from the broad-band absorption contribution, water-vapor temperature can then be calculated from the ratio of the integrated line areas as reported in Ref. [22]

$$T = \frac{(\frac{hc}{k})(E_2'' - E_1'')}{\ln(\frac{A_1}{A_2}) + \ln(\frac{S_2(T_0)}{S_1(T_0)}) + (\frac{hc}{k})(\frac{E_2''-E_1''}{T_0})}, \tag{1}$$

where k is the Boltzmann constant, h is Planck's constant, and c is the speed of light. A_1 and A_2 are the spectrally integrated areas (absorbances) of the absorption lines, E_1'' and E_2'' are the lower-state energies of both transitions, and $S_1(T_0)$ and $S_2(T_0)$ are the line strengths at reference temperature T_0 (296 K).

For the broad-band absorption in liquid water, the transmittance $\tau(\nu)$ at frequency ν of the NIR beam passing through the liquid is described by the Beer–Lambert equation

$$\tau(\nu) = (I_t/I_0)_\nu = a\exp(-n\sigma L), \tag{2}$$

where I_t and I_0 are the transmitted and incident intensities, respectively. L [cm] represents the length of the absorbing medium; and σ [cm^2/mol] is the absorption cross section, n [mol/cm^3] is the molar concentration of the species. The factor $a < 1$ attributes for the wavelength-independent signal losses. In order to discriminate the water film absorption from the other attenuation effects (represented by a), the ratio of transmittances $\tau(\nu)$ at two laser wavelengths was used. In this way, the effect of a cancels and the film thickness can be derived from (2) [13]

$$L = \frac{\ln(\tau(\nu_1)/\tau(\nu_2))}{(\sigma_2 - \sigma_1)n}, \tag{3}$$

where $\tau(\nu_1)$ and $\tau(\nu_2)$ are the transmittances at frequency ν_1 and ν_2, σ_1 and σ_2 are the corresponding spectral absorption cross sections. The absorption cross sections are those measured with the FTIR instrument.

3 Experimental setup

The experimental setup for liquid film absorption measurements is depicted in Fig. 2. The three fiber-pigtailed DFB diode lasers (NEL) are multiplexed into a single-mode fiber (9 µm core diameter) using a fiber combiner (Laser 2000). The diode laser assemblies were temperature and current controlled by a diode laser controller (ILX LDC-3908). A Faraday isolator (Laser 2000) was used to suppress back-scattering into the lasers by ∼ 50 dB. For fixed-wavelength spectroscopy the data sampling rate was 100 Hz. For scanned-wavelength operation, a function generator produced a saw-tooth signal for laser current tuning with a repetition rate of 100 Hz. The combined beams were sent through a collimator (Thorlabs F230FC-C), directed through the liquid layer, and collected in a multimode fiber (Thorlabs BFL37-400) by a second collimator. The signal was demultiplexed by a diffraction grating (Edmund) and then was focused onto three separate InGaAs photo diodes (Thorlabs PDA10CS-EC). Control of the experiment and further data processing was performed in a LabVIEW (National Instruments) environment.

A calibration tool (cf. insert in Fig. 2) was used to provide variable well-controlled film thicknesses in the 5–1000 µm range. The device consists of a stainless steel trough with a quartz window glued into its bottom, while a second quartz window, fixed in an adjustable mount, is positioned parallel above it by a translation stage. The trough is filled with water-provided liquid layers of well-defined thickness. The plate separation was measured by a caliper. Film-thickness measurements were performed in the range between approx. 0 (by placing both plates into contact) and 1000 µm with an accuracy of ±3 µm. To minimize etalon effects the laser beam was directed through the plates at an angle of 2° with respect to the plate normal. To vary the temperature of the liquid water, the calibration trough was wrapped with heating tape and the water temperature was measured with a thermocouple.

For the simultaneous measurements of liquid-film thickness and gas-phase temperature, scanned-wavelength spectroscopy was used. As discussed before, laser 1 was tuned in a wavelength range that is not absorbed by water vapor,

Table 2 Comparison of absorption cross-sections (cm^2/mol) of liquid water from literature [20] and from own FTIR measurements (cf. Fig. 1), respectively. Literature values are interpolated for the three wavelength positions given in Table 1

Laser	25°C		35°C		45°C		55°C	
	Literature	FTIR	Literature	FTIR	Literature	FTIR	Literature	FTIR
1	477.40	517.12	467.79	506.74	461.58	497.42	457.90	488.55
2	241.59	161.87	249.57	179.65	255.99	196.76	262.39	216.16
3	80.23	28.12	84.10	34.49	86.97	41.34	89.97	49.34

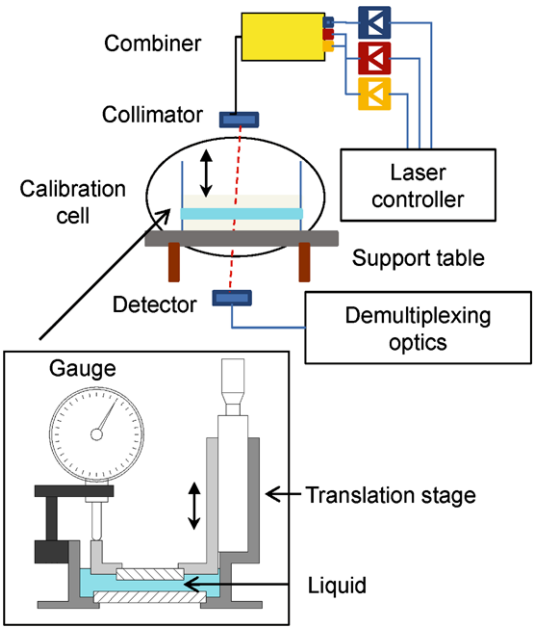

Fig. 2 Experimental setup for absolute film thickness measurements by multiplexed diode-laser absorption

whereas lasers 2 and 3 were tuned to the chosen water-vapor absorption lines for the determination of water-vapor temperature.

4 Results and discussion

Accurate absorption cross sections of liquid water are crucial for the quantitative determination of film thickness. Therefore, in Table 2 we present comparisons of absorption cross sections for the fixed wavelength positions of the three used diode lasers (given in Table 1) between interpolated values (cf. Fig. 5 in Ref. [20]) and calculated values from our own FTIR experiments (cf. Fig. 1) at four different fluid temperatures. The comparison shows a similar trend. There are no uncertainty limits given for the spectra presented in Ref. [20], however, judging from their limited spectral resolution, our measured absorption cross sections are more trusted. For the reference experiments, the measured transmittance at all three laser wavelengths for liquid film thicknesses (i.e., plate distances in the calibration tool) between 5 and 1000 µm, and at different film temperatures are plotted in Fig. 3a. The values are plotted in symbol at 45.6°C, whereas others are in lines. In accordance with Fig. 1, for a fixed film thickness the transmittance increases with decreasing wavelength of the three laser sources. Also, with increasing temperature the transmittance increases for laser 1 whereas for the other two lasers the opposite trend is observed. The variation of the absorption cross section with temperature at the wavelength of laser 1 and 2 are larger than that of lasers 3. Due to much weaker absorbance for laser 3, scattering of experimental data points around the expected exponential decrease with increasing layer thickness is large. Because lasers 1 and 2 show less noisy signal, the transmission ratio of these lasers at wavelengths off-resonant from any water vapor transitions was used to calculate the film thickness with the absorption cross sections depicted in Fig. 1. For repeated measurements the error in determining this ratio is less than 5% (RMS shown in Fig. 3a). Figure 3b shows the comparison between the calculated film thickness and the thickness determined in the reference measurements using the calibration tool. The deviation from the *best* value is around 3 and 7% (at the largest thickness), respectively. If the influence of water temperature is neglected an error of around 18% occurs when the temperature varies by 20 K. Future measurements will explore the correction for these effects using the simultaneous measurement of water temperature using the three-line absorption approach introduced above.

In the second experiment we demonstrate the simultaneous real-time measurement of liquid-fluid film thickness and water-vapor temperature above the liquid. A cylindrical box (diameter: 11 cm, height: 15 cm) with a transparent quartz plate as the bottom was used and a water film was applied to the bottom plate. A slow nitrogen purge flow was applied to avoid condensation on the other walls. The sending fiber was mounted in the top side of the box at 10 cm from the film. A nitrogen purge was applied between the back side of the plate and the lens-coupled detector fiber (cf. Fig. 2) to avoid spectral interference from water vapor in ambient air.

The liquid-film thickness as well as the water-vapor temperature above the film were determined using the described three-laser scanning scheme as a function of time while the plate was heated from its lower side by a heat gun to

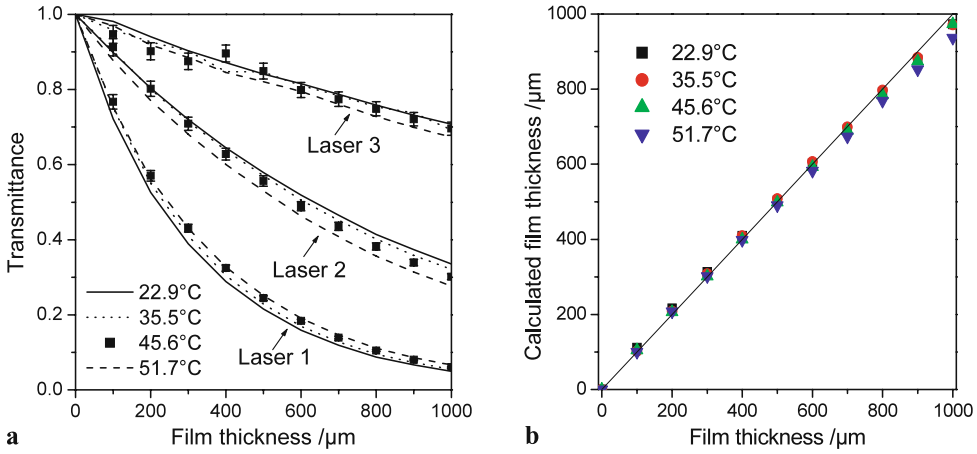

Fig. 3 (**a**) Transmittance at the selected three diode-laser wavelength positions (cf. Table 1) as a function of liquid film thickness. (**b**) Comparison of the calculated (from measured absorption cross sections) vs. the given (by the calibration tool) film thickness at different temperatures (*symbols*). The *solid line* represents the one-to-one correspondence between both values

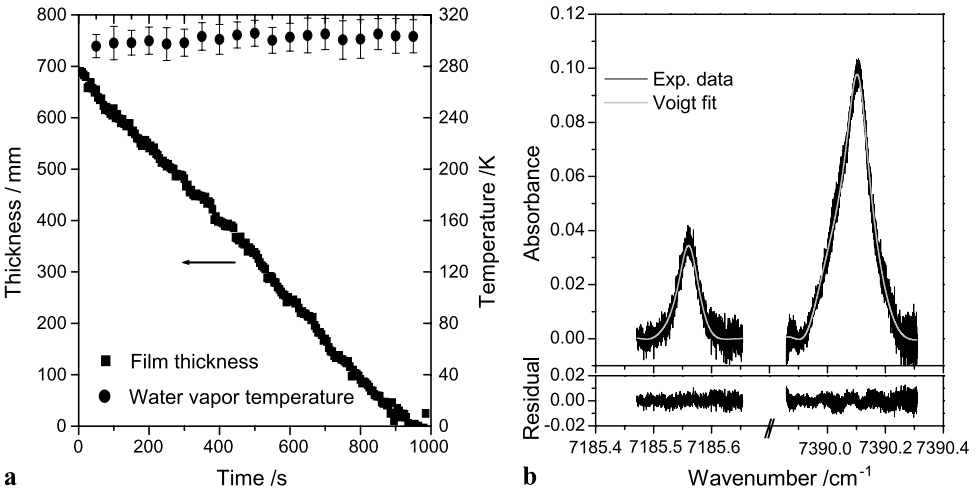

Fig. 4 (**a**) Film thickness variation and water-vapor temperature with time during the liquid-film evaporation. (**b**) Water-vapor absorption peaks; Voigt fit (*solid lines*) and corresponding residuals (*lower panel*) for the water-vapor lines accessed by laser 2 and 3, respectively

∼355 K. The liquid temperature was measured with a thermocouple to correct for the temperature dependence of the liquid–water absorption cross sections addressed by lasers 1 and 2, allowing for quantitative time-resolved liquid-film thickness measurements during film evaporation. Simultaneously, the water-vapor temperature was determined by two-line thermometry using lasers 2 and 3.

In Fig. 4a, the film thickness (solid squares) and vapor-phase temperature above the film (solid circles) are plotted versus time during the evaporation of a liquid–water droplet on the heated quartz plate. The initial film thickness of 700 µm decreased almost linearly during the 1000-s evaporation period. At the same time, within the measurement accuracy the vapor-phase temperature stayed almost constant. To not obscure the diagram, the temperature is plotted with less data points. The average temperature and the RMS for every 50 s are shown. To give an impression on the quality of the data, in Fig. 4b the water-vapor absorption lines scanned by lasers 2 and 3 shortly before the liquid film totally evaporated are presented together with their corresponding Voigt fits and fit residuals. Due to the slow evaporation from the liquid in this experiment water vapor is assumed to diffusively mix with surrounding air in thermal equilibrium, resulting in an almost constant temperature of about 300 K (±12 K) throughout the course of data recording. The temperature error bars mainly result from the limited signal-to-noise ratio due to the low water-vapor concentration.

5 Conclusions

A near-infrared diode laser absorption technique was employed to determine the thickness of the liquid film as well as water-vapor temperature above the liquid. The accuracy of the liquid layer thickness measurements was validated with defined liquid layers 5–1000 µm provided by a calibration tool with parallel quartz plates. Measurements were performed using three NIR diode lasers operating at different wavelengths between 1.35 and 1.47 µm within overtone vibrational bands of liquid water. Absolute absorption cross sections of liquid water were determined by FTIR measurements at the respective laser wavelengths for dif-

ferent temperatures and compared to interpolated literature values [20].

The technique was applied for simultaneous measurements of the liquid layer thickness and vapor phase temperature of evaporating a water droplet deposited on a heated quartz plate.

In a future work, through a proper choice of the three laser wavelengths, additionally to layer thickness and vapor temperature the online determination of the temperature of the liquid will be possible, which enables the on-line correction of water thickness measurements for the temperature-dependent absorption change within the liquid during film evaporation.

Acknowledgement Financial support by the German Research Foundation (DFG) within the framework of SFB 445 is gratefully acknowledged.

References

1. W. Hentschel, A. Grote, O. Langer, SAE Technical Paper, 972832 (1997)
2. M.C. Drake, T.D. Fansler, A.S. Solomon, J.G.A. Szekely, SAE Technical Paper, 2003-01-0547 (2003)
3. P.G. Felton, D.C. Kyritsis, S.K. Fulcher, SAE Technical Paper, 952464 (1995)
4. A.I. Petruchik, S.P. Fisenko, J. Eng. Phys. Thermophys. **72**, 43 (1999)
5. S. Wittig, J. Himmelsbach, B. Noll, H.J. Feld, W. Samenfink, J. Eng. Gas Turbines Power **114**, 395 (1992)
6. J.R. Mawhinney, J.K. Richardson, Fire Technol. **33**, 54 (1996)
7. J. Gieshoff, M. Pfeifer, A.S. Sindlinger, P. Spurk, G. Garr, T. Leprince, SAE Technical Paper, 2001-01-0514 (2001)
8. E.T. Hurlbert, T.A. Newell, Exp. Fluids **21**, 357 (1996)
9. T.A. Shedd, T.A. Newell, Rev. Sci. Instrum. **69**, 4205 (1998)
10. E. Kull, G. Wiltafsky, W. Stolz, K.D. Min, E. Holder, Opt. Lett. **22**, 645 (1997)
11. D. Greszik, H. Yang, T. Dreier, C. Schulz, in *Laser applications to chemical security and environmental analysis 2010, Technical Digest Opt. Soc. America* (2010)
12. A.A. Mouza, N.A. Vlachos, S.V. Paras, A.J. Karabelas, Exp. Fluids **28**, 355 (2000)
13. J.M. Porter, J.B. Jeffries, R.K. Hanson, Appl. Phys. B **97**, 215 (2009)
14. V.S. Wittig, J. Himmelsbach, M. Hallmann, W. Samenfink, A. Elsaesser, Motortech. Z. **55**, 160 (1994)
15. A.D. Griffiths, A.F.P. Houwing, Appl. Opt. **44**, 6653 (2005)
16. D.S. Baer, R.K. Hanson, M.E. Newfield, N.K.J.M. Gopaul, Opt. Lett. **19**, 1900 (1994)
17. J.T.C. Liu, G.B. Rieker, J.B. Jeffries, M.R. Gruber, C.D. Carter, T. Mathur, R.K. Hanson, Appl. Opt. **44**, 6701 (2005)
18. G.M. Hale, M.R. Querry, Appl. Opt. **12**, 555 (1973)
19. L. Kou, D. Labrie, P. Chylek, Appl. Opt. **32**, 3531 (1993)
20. J.R. Collins, Phys. Rev. **26**, 771 (1925)
21. D.W. Mattison, J.T.C. Liu, J.B. Jeffries, R.K. Hanson, AIAA-2005-0224 (2005)
22. X. Liu, J.B. Jeffries, R.K. Hanson, K.M. Hinckley, M.A. Woodmansee, Appl. Phys. B **82**, 469 (2006)